

Evolution of the surface roughness (dynamic scaling) and microstructure of sputter-deposited $\text{Ag}_{75}\text{Co}_{25}$ granular films

This article has been downloaded from IOPscience. Please scroll down to see the full text article.

2000 J. Phys.: Condens. Matter 12 9237

(<http://iopscience.iop.org/0953-8984/12/44/306>)

View [the table of contents for this issue](#), or go to the [journal homepage](#) for more

Download details:

IP Address: 171.66.16.221

The article was downloaded on 16/05/2010 at 06:56

Please note that [terms and conditions apply](#).

Evolution of the surface roughness (dynamic scaling) and microstructure of sputter-deposited $\text{Ag}_{75}\text{Co}_{25}$ granular films

R Mustafa Öksüzoglu†, Ayhan Elmali‡, Thomas E Weirich, Hartmut Fuess and Horst Hahn

Institute for Materials Science, Darmstadt University of Technology, Petersenstrasse 23, D-64287 Darmstadt, Germany

E-mail: hfuess@tu-darmstadt

Received 5 April 2000, in final form 20 July 2000

Abstract. X-ray specular-reflectivity measurements have been carried out on $\text{Ag}_{75}\text{Co}_{25}$ granular films which were sputter-deposited on Si substrates with SiO_2 surface, to investigate the evolution of surface roughness as a function of film thickness. X-ray reflectivity data were recorded for thicknesses of $\text{Ag}_{75}\text{Co}_{25}$ thin films ranging from 8.8–116.9 nm. A power law behaviour of the interfacial width of a growing interface in sputtered-deposited $\text{Ag}_{75}\text{Co}_{25}$ granular films was observed. The scaling exponent was found to be $\beta = 0.43 \pm 0.01$ and compared with theoretical calculations. High resolution electron microscopy revealed the presence of crystalline particles of fcc Ag and hcp Co. The structural and magnetoresistive properties of the films are discussed.

1. Introduction

The technological importance of thin films together with the interest in modelling thin film growth has stimulated many theoretical and experimental investigations [1–6]. It is generally accepted that the surface morphology and dynamics of a growing interface exhibit a simple dynamic scaling behaviour. In a dynamic scaling regime, the root-mean square (rms) surface roughness σ of a layer at a time t after the deposition started (or equivalently to the layer thickness d) is described by a power law: $\sigma \propto t^\beta \propto d^\beta$ [1]. The scaling exponent β depends predominantly on the mechanism of the film growth. Recently, this power law growth was observed for thin films in several single-component systems with evaporation and sputter techniques. Studies using thermal evaporation sources gave approximately consistent scaling exponents of $\beta \approx 0.25$ for iron [7, 8] and silver [9]. Sputter-deposition gave higher scaling exponents of $\beta = 0.40$ (at 300 K) and $\beta = 0.42$ (at 220 K) for Au films and of $\beta = 0.42$ at room temperature for Mo films [10, 11]. Collins *et al* [12] reported a considerably higher scaling exponent of $1 > \beta > 0.6$ for the growth of plasma polymer films from a plasma induced chemical vapour deposition at different deposition rates. For epitaxial growth of Si films on Si(001) from ultrahigh vacuum ion-beam sputter-deposition at 573 K a value of $\beta = 0.60$ was deduced by Lee *et al* [13]. In the past, theoretical and experimental studies focused mainly on the growth mechanism of one-component systems [1–6]. However, advanced materials in modern technology require the growth of at least two or even more components.

† Corresponding author. Tel.: +49-6151-16-2298; fax.: +49-6151-16-6023.

‡ Alexander von Humboldt Fellow, permanent address: Department of Engineering Physics, Faculty of Science, University of Ankara, 06100 Besevler, Ankara, Turkey.

Recently, Kotrla *et al* [14, 15] studied the dynamic scaling process for a 1+1-dimensional two-component system assuming a two-component single-step (TCSS) model derived from Monte Carlo simulations. In this model the process of particle deposition should be controlled by the energy change of the system from the previous deposition of a particle. A new particle can be added only at a growth site with local minimum in the surface height profile. Once the position and type of the particle are selected, they are permanently fixed. The energy is suitably described by an Ising-like interaction. Although the dynamic scaling process on 1+1-dimension for a two-component system was theoretically described, no experimental proof for a dynamic scaling process of a two-component system exists until now. In this paper, the dynamic scaling process of sputter-deposited Ag₇₅Co₂₅ granular films was investigated by *ex situ* x-ray reflectivity measurements. Our purpose was to experimentally check the power law and to determine the scaling exponent for sputter-deposited granular thin films by using x-ray specular-reflectivity. AgCo granular films have potential technological importance due to their giant magnetoresistance (GMR) effects [16–18]. The AgCo system was chosen as a model system since cobalt and silver do not form intermetallic compounds and are immiscible in all portions. We have also investigated the microstructure of AgCo thin films as the microstructure of AgCo films is still controversially discussed. The principle difficulty is to define the structure of the Co particle (fcc or hcp). Li *et al* [19] studied the microstructure of Ag₇₅Co₂₅ films using high resolution transmission electron microscopy (HRTEM) and found that the size of the Co particle is in the order of about 1.5 nm. However, no clear evidence for the structure of Co particles was found. Ounadjela *et al* [20] studied the microstructure of MBE deposited Ag₅₇Co₄₃ films using HRTEM and found that the size of Co particles ranges from 1–2 nm in the hexagonal structure. In this paper, the microstructure of the sputter-deposited Ag₇₅Co₂₅ films were characterized by x-ray diffraction and HRTEM.

2. Experimental details

The samples investigated were prepared at room temperature by dc magnetron-sputtering onto Si substrates with a 100 nm SiO₂-buffer layer. The target materials were 99.9% purity Co and Ag (K J Lesker Company, UK). The argon pressure during the preparation of the films was adjusted at 7.5 mTorr by a gas-flow controller. The base pressure was more than 1×10^{-7} Torr. The sample thickness and the composition of the films were determined by calibrated quartz crystal monitors. The deposition rates were 3.0 \AA s^{-1} for Ag and 1.0 \AA s^{-1} for Co, respectively (nominal composition Ag₇₅Co₂₅). The specular reflectivity scans were performed on a four-circle diffractometer system (Seifert XR 3000 HR) equipped with a double Ge(220) monochromator (horizontal divergence $\Delta\Theta_h \approx 0.0033^\circ$) and scatter-slits in front of the sample and the detector. The distance from the centre of the sample to the detector was 200 mm, and the receiving slit geometry defined a scattering resolution of $\Delta\Theta \approx 0.014^\circ$. Furthermore, the structure of the film was investigated by grazing incidence x-ray diffractometry (GIXD). A Bragg–Soller x-ray diffractometer system with a flat secondary monochromator and fixed CuK α tube (Seifert XRD 3000 TT) was used at low incidence ($\Omega = 1^\circ$) with 2Θ scan. The microstructure of the first mechanical and later ion thinned samples was investigated in a Jeol 3010UHR transmission electron microscope operated at 300 kV. High resolution electron microscopy (HREM) images and selected area electron diffraction (SAED) patterns were recorded from thin sample areas on film and later digitized with a video CCD camera (Dage MIT, model CCD72E) for image analysis by the CRISP and ELD program (Calidris, Sollentuna, Sweden). The Magnetoresistance (MR) ratio $\Delta R/R$ was measured by a standard four terminal dc technique with the magnetic field perpendicular to the sample current. Both the magnetic field and sample current were adjusted parallel to the film plane.

3. Results and discussion

3.1. Characterization of the samples

The x-ray diffraction pattern of an as-deposited $\text{Ag}_{75}\text{Co}_{25}$ film in a different thickness (from 8.8–188.5 nm) is shown in figure 1. Scattering patterns exhibit single phase fcc peaks of Ag for all samples. Despite the strong tendency for phase separation in this system, neither fcc or hcp Co was detected by the x-ray experiments in all films. Xiao *et al* [21] investigated the structure of sputter-deposited $\text{Ag}_{80}\text{Co}_{20}$ films by x-ray experiments. Their samples showed a second set of fcc diffraction peaks after annealing from 200–605°, which indicated the formation of small fcc Co particles embedded in fcc Ag.

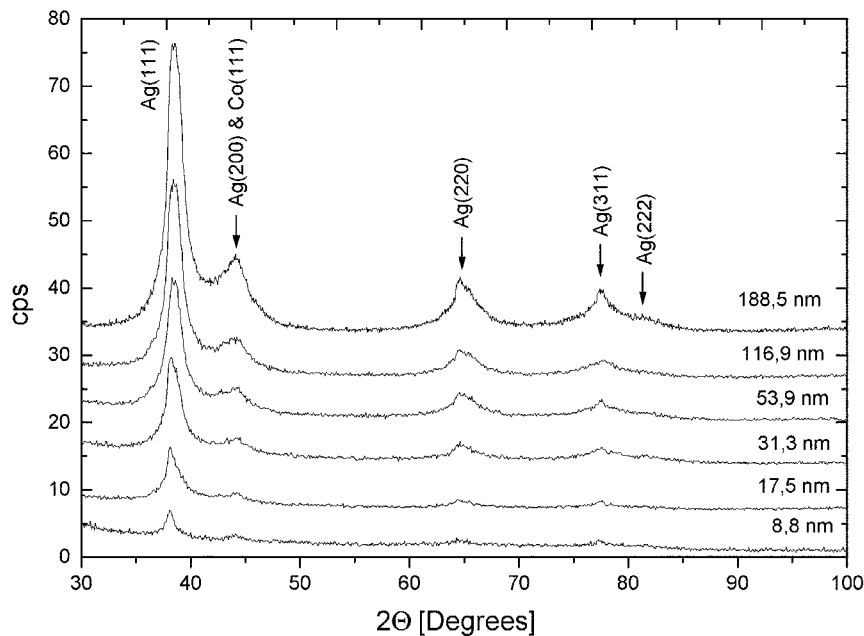
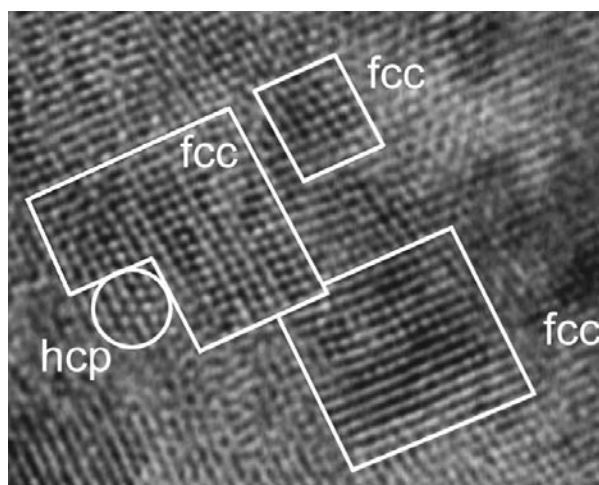


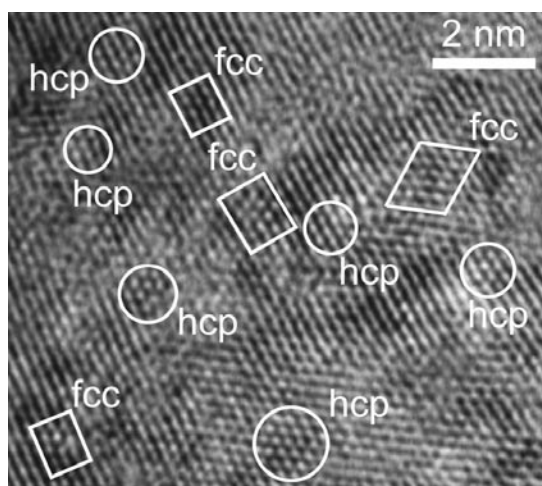
Figure 1. X-ray diffraction of all as-deposited $\text{Ag}_{75}\text{Co}_{25}$ granular films with thickness from 8.8–188.5 nm

A representative HREM image of a very thin sample area is shown in figure 2. The HREM image was taken under defocus conditions so that all columns of atoms appear with the same contrast (*Scherzer* defocus). Hence a straightforward interpretation of the image is possible since all atom positions are represented by black spots. Fourier transforms (FT) of the calibrated HREM images show crystalline reflections around $0.42\text{--}0.53 \text{ \AA}^{-1}$ (corresponding to 2.4 \AA and 1.9 \AA in real space). This is in good agreement with Ag(111), Ag(200), Co(111) in fcc phase and Co(100), Co(101) in hcp phase. The contribution of amorphous surface layers was removed from the image by quasi-optical filtering in Fourier-space using the above indicated spatial frequencies and subsequent calculation of the inverse FT. Analysis of the filtered images permitted us to easily identify and estimate the size of individual particles. The non-uniform radial distribution of the reflections in the FT of the HREM images indicates a high degree of preferred orientation fcc Ag(111). This is also supported by SAED (figure 3). However, due to the strong corrugation of the sample only a small fraction of the crystallites can be almost exactly oriented along the prominent directions at a time. Nevertheless, it was possible to

distinguish several individual particles and identify fcc Ag in projection along the [100] and [110] direction and hcp Co along [001]. For illustration some of the areas showing prominent orientations are marked in figure 2. The size of the fcc Ag particles, as estimated from the HREM images, ranges from 15–40 Å while the size of the hcp Co particles is significantly smaller at about 10–15 Å. Analysis of the SAED patterns showed the dominant contribution of fcc Ag to the pattern (see figure 3). Some faint reflection rings arising from hcp Co(100) and hcp Co(−110) could also be found.



(a)



(b)

Figure 2. The HREM images of some typical areas showing hcp (circle) and fcc (rectangle) orientations (see text).

The magnetoresistance (MR) of the samples was measured at room temperature. Figure 4 shows the MR ratios ($\Delta R/R = (R(H) - R(0))/R(0)$) of the prepared films. Heterogeneous alloys are complex systems and there are many factors which effect both the maximum value of GMR and its variation with applied field. For two given materials, the GMR effect is known to depend on the concentration of magnetic metal and shape and the size

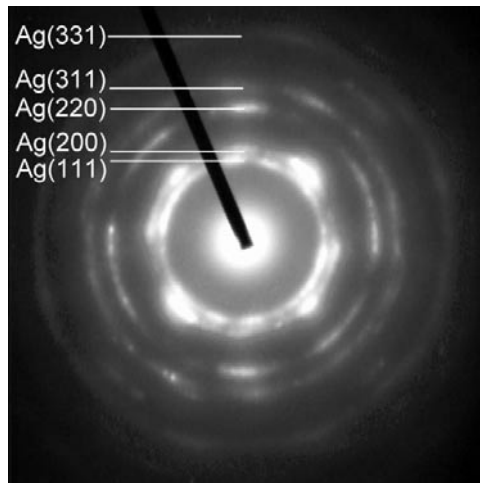


Figure 3. SAED pattern of the investigated sample, with diffraction lines of fcc Ag.

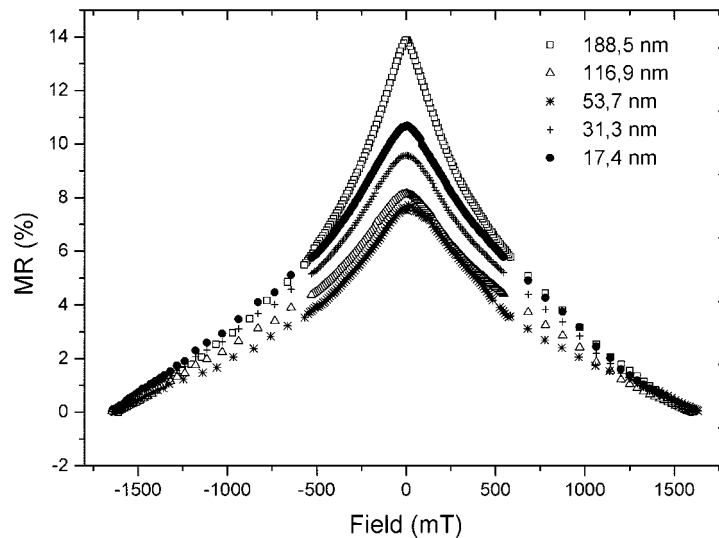


Figure 4. Thickness dependence of magnetoresistance for $\text{Ag}_{75}\text{Co}_{25}$ granular films.

and distribution of magnetic grain. The MR raises from 7.7–13.9% with increasing film thickness from 17.4–188.5 nm. A similar result was obtained in a previous investigation on sputter-deposited $\text{Ag}_{73}\text{Co}_{27}$ films of thickness below 200 nm [22].

3.2. Growth mechanism

After the preparation of the samples, the *ex-situ* specular reflectivity measurements were immediately carried out. Figure 5 shows the specular reflectivity measurements for different $\text{Ag}_{75}\text{Co}_{25}$ film thicknesses ranging from 8.8–116.9 nm. Oscillations in the curve emerge from interference of the reflected beam at the AgCo–air interface (i.e. the AgCo–film surface)

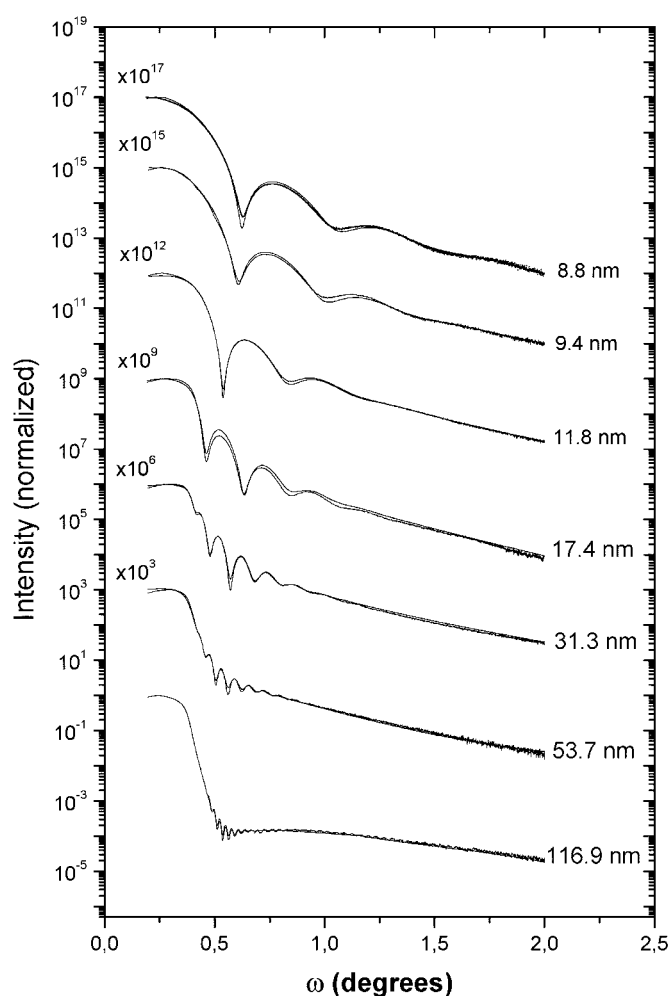


Figure 5. Specular-reflectivity curves for $\text{Ag}_{75}\text{Co}_{25}$ films, in thickness from 8.8–116.9 nm. The solid lines are the results of the fits.

and the beam reflected at the AgCo–substrate interface. The oscillation period is inversely proportional to the AgCo thickness. The amplitude contains information on the interfacial widths (σ) of the two interfaces. For thick films the interference fringes disappear due to finite instrumental resolution and roughness.

The data were fitted using Parrat's algorithm for the reflectivity [23] with the Névo–Croce formula for interface roughness [24]. The best fits were shown as solid lines in figures 5. The fitting parameters were layer thickness, roughness and densities associated with each layer. Figure 6(a) shows the roughness evolution of the surface and of the $\text{Ag}_{75}\text{Co}_{25}/\text{SiO}_2$ interface obtained from the fitted reflection curves. The scaling exponent β was determined from evolution of the roughness of the $\text{Ag}_{75}\text{Co}_{25}$ –air interface dependent on the film thickness, $\sigma \propto d^\beta$. The corresponding scaling exponent is $\beta = 0.43 \pm 0.01$ (figure 6(b)). The value of σ presented in figure 6(a) was corrected for the rms roughness of the SiO_2 -buffer layer σ_s , according to the relation $\sigma_c = (\sigma^2 - \sigma_s^2)^{1/2}$. This correction alters the value of β by about 0.03.

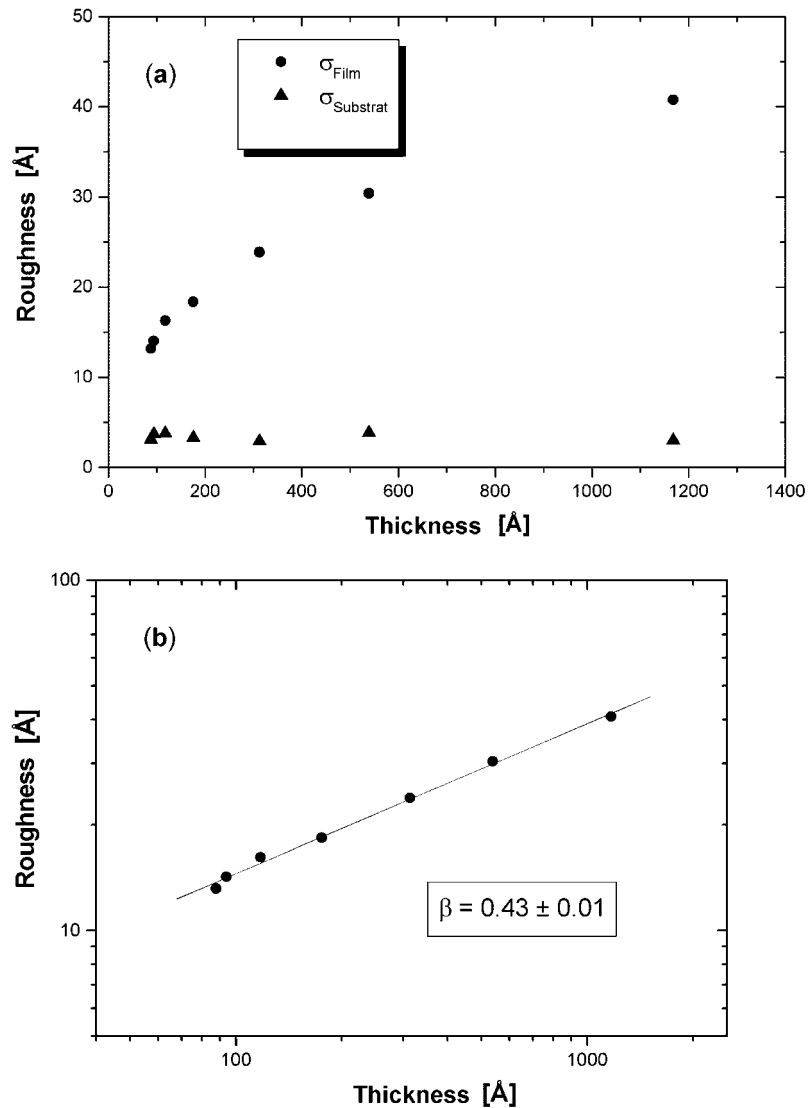


Figure 6. The roughness evolution of surface and of the $\text{Ag}_{75}\text{Co}_{25}/\text{SiO}_2$ interface obtained from the fits of the data (a). The evolution of the surface roughness plotted in a log-log scale (b). The slope of the curve corresponds to the scaling exponent β .

Many of the previous investigations of one-component growth mechanisms are based on the Kardar–Parisi–Zhang (KPZ) universality class [2]. In previous experimental studies of the deposition of thin films, the scaling exponents of metals were found to be $0.22 < \beta < 0.56$ [8, 25]. Studies using thermal evaporation sources gave approximately consistent scaling exponents of $\beta \approx 0.25$ for iron [7, 8] and silver [9] and the value obtained for the exponent β is within experimental error of the KPZ value. The value $\beta = 0.43$ of the present study is in agreement with the scaling exponents for sputter-deposited gold and molybdenum films [10, 11]. But, these values are substantially larger than 0.25 which was predicted by the KPZ equation for the 2+1 system. In the simple random deposition there is no spatial or temporal

correlation between the deposited particles (the extreme kinetic limit) and the exponent β is 0.5. The particles simply fall until they reach the top of the column in which they were dropped or they reach the substrate [26]. At this point they stop and become part of the aggregate. Collins *et al* [12] found $1 > \beta > 0.6$ from a plasma induced chemical vapour deposition process at different deposition rates. Models including surface pinning and shadowing may lead to $\beta > 0.5$ [27]. The quantity β is related to long-range feature and is strongly dependent on film deposition techniques. There might be some inner relations between β and deposition techniques during the nonequilibrium dynamics of interface growth. The comparison of the results of the sputter-deposited films to studies based on the KPZ equation indicates that the description of experimental growth systems such as sputter deposition may require additional mechanisms beyond the KPZ equation.

For a two-component system only Kotrla *et al* [14, 15] proposed dynamic scaling by a (1+1)-dimensional TCSS model and found that the scaling exponent should vary with the coupling strength between two different kinds of particles. We cannot directly compare our result with a (1+1)-dimensional TCSS model since our system is in a (2+1)-dimension. For sufficiently strong coupling the TCSS model predicts an intermediate growth regime with a new scaling exponent $\beta = 0.5$ and the scaling exponent should continuously increase with the coupling. When the coupling becomes weak, the evolution of the surface roughness is expected to be the same as in the ordinary one-component growth model. Our result may also indicate that the coupling strength between Ag and Co particles is not strong in $\text{Ag}_{75}\text{Co}_{25}$ since the scaling exponent for the sputter-deposited $\text{Ag}_{75}\text{Co}_{25}$ film is almost equal to the scaling exponent for sputter-deposited gold and molybdenum films.

To conclude, we investigated the evolution of the surface roughness of $\text{Ag}_{75}\text{Co}_{25}$ films grown on SiO_2 -buffer layers by x-ray reflectivity measurements. We observed the power law behaviour of the interfacial width of a growing interface in sputtered-deposited $\text{Ag}_{75}\text{Co}_{25}$ granular film. The scaling exponents β observed on the growth of $\text{Ag}_{75}\text{Co}_{25}$ films amount to 0.43 ± 0.01 . The MR of granular films $\text{Ag}_{75}\text{Co}_{25}$ has been found to increase considerably with the increase of film thickness. The maximum value of MR observed in as-deposited $\text{Ag}_{75}\text{Co}_{25}$ is 13.9%. Studies of the films with HRTEM showed that these $\text{Ag}_{75}\text{Co}_{25}$ films consist of ultra-fine Co grains in the hcp phase with an average grain size about 10–15 Å and Ag grains in the fcc phase with an average grain size 15–40 Å.

4. Acknowledgments

RMÖ thanks the Ministry of Education, Republic of Turkey, for the financial support of his PhD studies. AE is grateful to the Alexander von Humboldt Foundation Bonn, Germany, for a Research Fellowship. Financial support from the Fonds der Deutschen Chemischen Industrie is gratefully acknowledged.

5. References

- [1] Family F and Vicsek T 1985 *J. Phys. A: Math. Gen.* **18** L75
- [2] Kardar M, Parisi G and Zhang Y-C 1986 *Phys. Rev. Lett.* **56** 889
- [3] Chiarello R, Panella V, Krim J and Thompson C 1991 *Phys. Rev. Lett.* **67** 3408
- [4] Kahanda G L M K S, Zou X, Farrell R and Wong P 1992 *Phys. Rev. Lett.* **68** 3741
- [5] Krug J 1997 *Adv. Phys.* **46** 139
- [6] Levi A C and Kotrla M 1997 *J. Phys.: Condens. Matter* **9** 299
- [7] Chevier J, Le Thanh V, Buys R and Derrien J 1991 *Europhys. Lett.* **16** 737
- [8] He Y-L, Yang H-N, Lu T-M and Wang G-C 1992 *Phys. Rev. Lett.* **69** 3770
- [9] Thompson C, Palasantzas G, Feng Y P, Sinha S K and Krim J 1994 *Phys. Rev. B* **49** 4902

- [10] You H, Chiarello R P, Kim H-K and Vandervoort K G 1993 *Phys. Rev. Lett.* **70** 2900
- [11] Jun Wang, Gang Li, Ping Yang, Mingqi Cui, Xiaomung Jiang, Bing Dong and Hong Liu 1998 *Europhys. Lett.* **42** 283
- [12] Collins G W, Letts S A, Fearon E M, McEachern R L and Bernat T P 1994 *Phys. Rev. Lett.* **73** 708
- [13] Lee N-E, Cahill D G and Greene J E 1996 *Phys. Rev. B* **53** 7876
- [14] Kotrla M and Predota M 1997 *Europhys. Lett.* **39** 251
- [15] Kotrla M, Slanina F and Predota M 1998 *Phys. Rev. B* **58** 10 003
- [16] Carey M J, Young A P, Starr A, Rao D and Berkowitz A E 1992 *Appl. Phys. Lett.* **61** 2935
- [17] Barnard J A, Waknis A, Tan M, Haftek E, Parker M R and Watson M L 1992 *J. Magn. Magn. Mater.* **94** L1
- [18] Wang J-Q and Xiao G 1994 *Phys. Rev. B* **49** 3982
- [19] Li Z-G, Wan H, Liu J, Tsoukatos A, Hadjipanayis G C and Liang L 1993 *Appl. Phys. Lett.* **63** 3011
- [20] Ounadjela K, Thompson S M, Gregg J F, Azizi A, Gester M and Deville J P 1996 *Phys. Rev. B* **54** 12252
- [21] Xiao J Q, Jiang J S and Chien C L 1992 *Phys. Rev. B* **46** 9266
- [22] Mitchell J R and Berkowitz A E 1994 *J. Appl. Phys.* **75** 6912
- [23] Parratt L G 1954 *Phys. Rev.* **95** 359
- [24] Nénot L and Croce P 1980 *Rev. Phys. Appl.* **15** 761
- [25] Ernst H-J, Fabre F, Folkerts R and Lapujoulade J *Phys. Rev. Lett.* **72** 112
- [26] Family F 1986 *J. Phys. A: Math. Gen.* **19** L441
- [27] Jensen M H and Procaccia I 1991 *J. Physique* **1** 1139